

Nanobody-Enhanced Targeting of AAV Gene Therapy Vectors

Anna Marei Eichhoff,^{1,2} Kathleen Börner,^{3,4,5} Birte Albrecht,¹ Waldemar Schäfer,¹ Natalie Baum,¹ Friedrich Haag,¹ Jakob Körbelin,⁶ Martin Trepel,⁶ Ingke Braren,⁷ Dirk Grimm,^{3,4,5} Sahil Adriouch,^{1,2} and Friedrich Koch-Nolte¹

¹Institute of Immunology, University Medical Center Hamburg-Eppendorf, Hamburg, Germany; ²Institute for Research and Innovation in Biomedicine, INSERM U1234, Normandy University, Rouen, France; ³Department of Infectious Diseases/Virology, Heidelberg University Hospital, Heidelberg, Germany; ⁴BioQuant, Heidelberg University, Heidelberg, Germany; ⁵German Center for Infection Research, Heidelberg, Germany; ⁶Center for Oncology, University Medical Center Hamburg-Eppendorf, Hamburg, Germany; ⁷Institute of Pharmacology, University Medical Center Hamburg-Eppendorf, Hamburg, Germany

A limiting factor for the use of adeno-associated viruses (AAVs) as vectors in gene therapy is the broad tropism of AAV serotypes, i.e., the parallel infection of several cell types. Nanobodies are single immunoglobulin variable domains from heavy chain antibodies that naturally occur in camelids. Their small size and high solubility allow easy reformatting into fusion proteins. Herein we show that a membrane protein-specific nanobody can be inserted into a surface loop of the VP1 capsid protein of AAV2. Using three structurally distinct membrane proteins—a multispans ion channel, a single-span transmembrane protein, and a glycosylphosphatidylinositol (GPI)-anchored ectoenzyme—we show that this strategy can dramatically enhance the transduction of specific target cells by recombinant AAV2. Moreover, we show that the nanobody-VP1 fusion of AAV2 can be incorporated into the capsids of AAV1, AAV8, and AAV9 and thereby effectively redirect the target specificity of other AAV serotypes. Nanobody-mediated targeting provides a highly efficient AAV targeting strategy that is likely to open up new avenues for genetic engineering of cells.

INTRODUCTION

Adeno-associated viruses (AAVs) are established as gene therapy vectors.^{1–3} AAVs are small 20- to 25-nm, non-enveloped, 4.7-kb single-stranded DNA viruses with an icosahedral 60-mer capsid. In non-replicative recombinant AAVs designed for gene delivery to a target cell, the nucleotide sequence to be delivered replaces the viral capsid and replication genes.^{4–6} The delivered nucleotide sequence may encode, for example, a fluorescent reporter, a replacement for a defective cellular gene, a protein or RNA modulator of a specific cellular function, or a toxin/suicide factor.

A limiting factor for successful gene delivery by AAV vectors is the broad tropism of the common AAV serotypes.⁷ Targeting technologies aim to direct the AAV capsid to specific cell surface receptors,^{8,9} e.g., by genetic fusion or chemical ligation of the ligand for a cell surface receptor to a capsid protein.^{10–12} The 3D structures of different AAV serotypes have provided a rational basis for eliminating binding to ubiquitously expressed receptors and for inserting a peptide or a

protein domain into an exposed loop of the viral capsid.^{13–15} For example, mutation of two arginine residues in the GH12/GH13 loop (R585, R588) to alanine abolishes binding of AAV2 to heparan sulfate proteoglycan (HSPG).^{16,17} Insertion of synthetic peptide libraries in this region followed by selection of specifically transduced cells or tissues has yielded AAV variants with improved target specificities.^{9,18–22}

Owing to their exquisite specificity, antibodies are potential targeting moieties. The large size and tetrameric format of antibodies, however, have hampered their use for targeting of AAVs.^{10,23} Nanobodies—single VH domains from camelid heavy chain antibodies—provide high specificity and stability.²⁴ Their small size and high solubility allow easy reformatting into fusion proteins.^{24–26} We have previously generated nanobodies against structurally distinct cell surface proteins, including CD38, a single span transmembrane protein, ARTC2.2, a glycosylphosphatidylinositol (GPI)-anchored ectoenzyme, and P2X7, a homotrimeric ion channel (Figure 1A).^{27–29} These nanobodies specifically recognize stably transfected HEK cells expressing the cognate target protein (Figure 1B). We hypothesized that these membrane protein-specific nanobodies could be used to manipulate the cellular specificity of AAVs with molecular precision. To this end, we inserted the membrane protein-specific nanobody into a surface loop of the VP1 viral capsid protein, i.e., a position that had previously been shown to accommodate the fluorescent protein mCherry (Figure 1C).³⁰ Our results demonstrate that display of a membrane protein-specific nanobody on the AAV capsid effectively enhances its capacity to transduce specific target cells. We show that this flexible strategy is readily adapted to a broad range of AAV serotypes and to different membrane proteins. Our results open up a new avenue for targeted gene delivery into specific cell types.

Received 15 August 2019; accepted 10 September 2019;
<https://doi.org/10.1016/j.omtm.2019.09.003>.

Correspondence: Friedrich Koch-Nolte, Institute of Immunology, N27, University Medical Center Hamburg-Eppendorf, Martinistrasse 52, 20246 Hamburg, Germany.

E-mail: nolte@uke.de



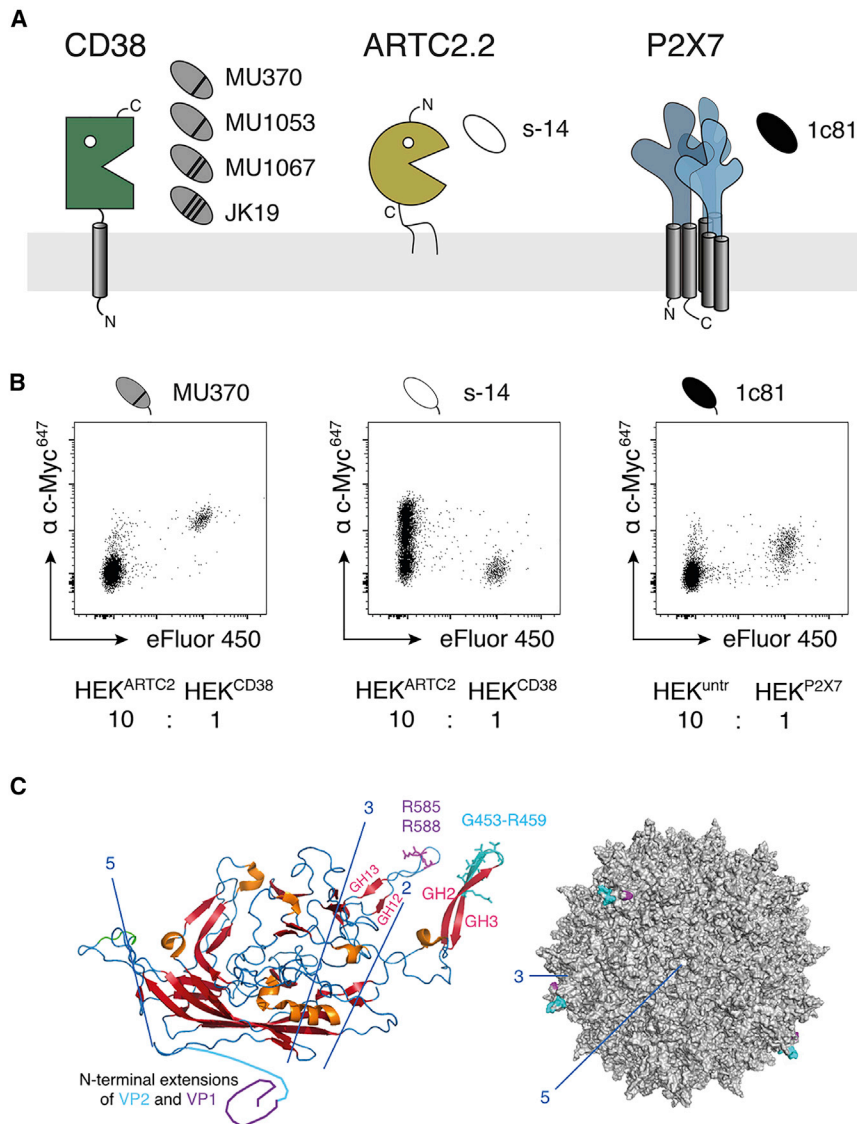


Figure 1. Schematic Diagram of the Three Membrane Proteins and Their Cognate Nanobodies Used in This Study for the Directed Targeting of AAVs

(A) CD38 is a type II single span transmembrane protein, ARTC2.2 is a GPI-anchored ectoenzyme, and P2X7 is a multispan homotrimeric ion channel. The CD38-specific nanobodies used here recognize three nonoverlapping epitopes, indicated by the slanted black lines. (B) Paired samples of untransfected HEK cells and HEK cells stably transfected with CD38, ARTC2.2, or P2X7 were mixed at a 10:1 ratio after one of the cell samples had been labeled with eFluor 450 before mixing. Cells were incubated with c-Myc-tagged ARTC2.2-specific, CD38-specific, or P2X7-specific nanobodies for 30 min at 4°C. Cells were washed and bound nanobodies were detected with Alexa Fluor 647 fluorochrome-conjugated c-Myc-specific mAb 9E10 by flow cytometry. (C) Ribbon drawing of the VP1 capsid protein and space fill models of AAV2^{RA} illustrating the nanobody insertion site in the GH2/GH3 loop (cyan). Beta sheets are indicated in red, α helices in orange. The two arginine residues in the GH12/GH13 loop that were replaced by alanine to inhibit binding to HSPG are indicated in magenta. Regions corresponding to the N-terminal extensions of VP2 and VP1 are indicated schematically by light blue and purple lines. These are not visible in any of the known AAV crystal structures. The locations of the symmetry axes are indicated in blue. Figures were assembled in PyMOL using coordinates of the 3D structure of AAV2 (PDB: 1LP3).¹³

To ensure that recombinant AAVs produced in transfected HEK cells contained only nanobody-VP1 capsid proteins—i.e., only one to five copies per particle—we used two distinct capsid-protein encoding plasmid vectors. The vector encoding the VP1-Nb fusion contains a mutated splice acceptor (sa) for the common VP2/VP3 mRNA, preventing production of any VP2-Nb or VP3-Nb fusions (Figure 2A). The vector encoding unmodified VP2 and VP3

contains a mutated start codon (sc) of the VP1 coding sequence, preventing production of unmodified VP1 (Figure 2A). Recombinant nanobody-displaying AAV2^{RA} were generated in cotransfected HEK cells and were analyzed for incorporation of the VP1-Nb fusion protein by western blot analyses using monoclonal antibody (mAb) B1 that recognizes a common epitope in the capsid proteins (Figure 2B).³¹ The results confirm that the recombinant AAV incorporated Nb-VP1 fusion proteins. The latter show the expected increase in apparent molecular mass by ~15 kDa compared to unmodified VP1 in the parental AAV2^{RA} (Figure 2B).

Next, we evaluated the specific binding of nanobody-displaying AAV2^{RA} to HEK cells stably transfected with CD38, ARTC2.2, or P2X7, i.e., the membrane proteins used here as targeted AAV receptors, by flow cytometry using mixtures of transfected and untransfected

RESULTS

The GH2/GH3 Loop of the VP1 Capsid Protein of AAV2 Readily Accommodates the Insertion of a Membrane Protein-Specific Nanobody

Figure 2 illustrates our strategy to retarget AAV vectors by inserting one to five copies of a membrane protein-specific nanobody into the viral capsid. As the insertion site, we chose the most prominent protrusion of the capsid, i.e., the GH2/GH3 loop of VP1 (Figure 2A).^{13,30} To this end, we genetically replaced 7 amino acids (aa) of this loop in AAV2 (amino acids 453–459) by 110–130 aa residues of a nanobody. In order to allow for flexibility and to direct the paratope of the nanobody away from the capsid, we flanked the nanobody at its N and C termini with long and short peptide linkers, respectively. To prevent binding to HSPG, we mutated R585 and R588 in the adjacent surface loop GH12/GH13 to alanine, yielding AAV2^{RA}.^{16,17}

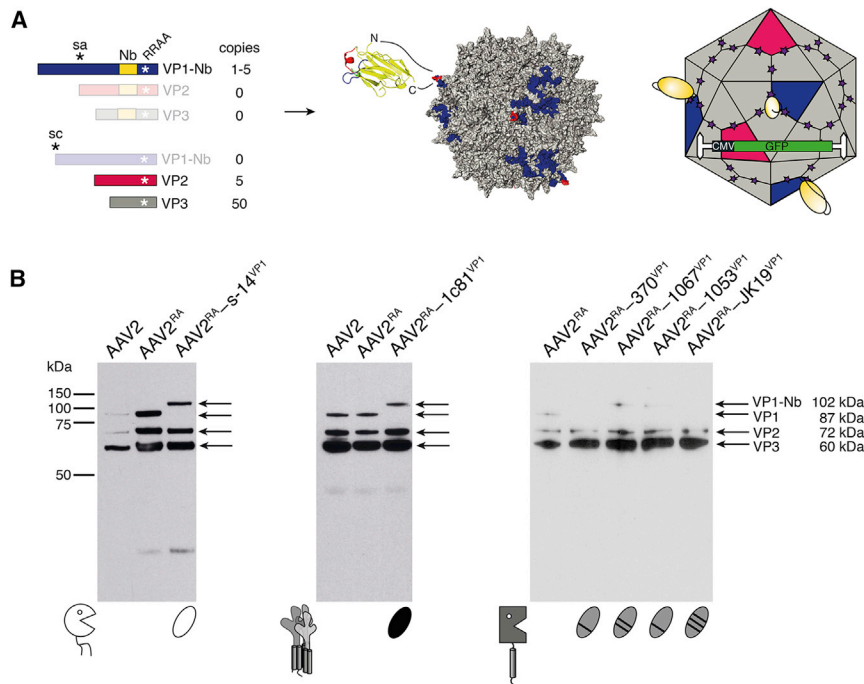


Figure 2. Membrane Protein-Specific Nanobodies Are Readily Incorporated into AAV Capsids and Mediate Specific Binding of Recombinant AAV to Target-Expressing Cells

(A) VP1 (blue), VP2 (magenta), and VP3 (gray) assemble the viral capsid in a ratio of 5:5:50. We genetically fused the nanobody (yellow) into the GH2-GH3 surface loop of VP1 (see Figure 1C) and mutated arginines R585 and R588 to alanine (indicated by white asterisks). In the plasmid encoding the VP1-Nb fusion, the splice acceptor (sa) was inactivated to prevent incorporation of the nanobody into VP2 and VP3. Expression of unmodified VP2 and VP3 was directed by a second plasmid, in which the start codon (sc) of VP1 was inactivated to prevent incorporation of unmodified VP1. A GFP expression cassette was used as reporter (green). (B) GFP-encoding parental AAV2 and recombinant nanobody-displaying AAV2^{RA} were produced in transfected HEK cells. Cells were harvested 72 h after transfection, and proteins in cell lysates were analyzed by western blotting using mAb B1 that recognizes a common epitope near the C terminus of all capsid proteins. The respective target membrane protein and the nanobody incorporated into the VP1-Nb fusion protein are indicated schematically below the blots using the same icons as in Figure 1A.

HEK cells (Figure 3). Bound AAV particles were detected with a fluorochrome-conjugated heavy chain antibody, derived from AAV2-specific mAb A20.^{14,31} The results confirm specific binding of nanobody-displaying AAV to HEK cells transfected with the respective target antigen and little if any binding to untransfected HEK cells.

Insertion of a Membrane Protein-Specific Nanobody into VP1 Specifically Enhances Transduction of HEK Cells Stably Transfected with the Respective Target Protein

In order to determine whether nanobody-displaying AAV2^{RA} improve the transduction of target-expressing cells, we incubated untransfected and stably transfected HEK cells with titrated doses of GFP-encoding AAV2^{RA} and analyzed the cells 48 h later by flow cytometry (Figure 4). We observed strongly enhanced GFP expression by HEK cells expressing the cognate antigen for each of the three target proteins analyzed. GFP expression was most strongly enhanced (>500-fold) for HEK cells expressing the multispans P2X7 ion channel (Figure 4A) and least strongly for cells expressing the GPI-anchored ARTC2.2 ectoenzyme (Figure 4B).

The Nanobody-VP1 Fusion of AAV2^{RA} is Readily Incorporated into the Capsid of other AAV Serotypes, and it Thereby Redirects the Target Specificity of the Mosaic AAV

To determine whether the nanobody-based targeting strategy could be adapted also to other AAV serotypes, we took advantage of the capacity of AAV capsid proteins to assemble into mosaic capsids (illustrated schematically in Figure 5A).³² To ensure that mosaic AAV particles contained only 1–5 VP1-Nb capsid proteins of AAV2^{RA} and 55–59 VP2/VP3 capsid proteins of a different AAV serotype, we introduced a premature stop codon into the VP1 coding sequence on the rep-cap

plasmids of AAV8, AAV9, and AAV1P5 (containing a 9-aa insertion in the GH12/GH13 loop; see Materials and Methods). Co-transfection of HEK cells with these plasmids and the plasmid encoding a nanobody inserted into VP1 of AAV2^{RA} (with inactivated splice signal for VP2/VP3) yielded mosaic AAV8, AAV9, or AAV1P5 virions. All nanobody-displaying mosaic AAVs specifically enhanced the transduction of HEK cells expressing the cognate target (Figure 5B).

We next analyzed whether nanobody-displaying mosaic AAV could also enhance transduction of other cells (Figure 6). CA46 is a human B cell lymphoma that endogenously expresses CD38, and Yac-1 is a mouse T cell lymphoma that endogenously expresses P2X7. Integration of the CD38-specific VP1-Nb capsid protein of AAV2^{RA} into the capsids of AAV8, AAV9, or AAV1P5 resulted in effective transduction of CA46 cells but not Yac-1 cells (Figures 6A and 6B). Conversely, integration of the P2X7-specific VP1-Nb capsid protein of AAV2^{RA} into the capsids of other serotypes resulted in effective transduction of Yac-1 but not CA46 cells (Figure 6C). We also assessed whether mosaic AAV1P5 could enhance the transduction of myeloma cells in a human bone marrow sample containing a distinct population of CD38^{hi}/CD138^{hi} myeloma cells (~15% of cells) (Figure 6D). The results demonstrate that AAV1P5 displaying a CD38-specific nanobody indeed mediate robust and specific transduction of myeloma cells whereas AAV1P5 displaying a P2X7-specific nanobody did not (Figure 6D).

DISCUSSION

The goal of this study was to use nanobody technology to redirect the cellular tropism of recombinant AAVs by inserting a membrane protein-specific nanobody into the exposed GH2/3 loop of VP1. Our

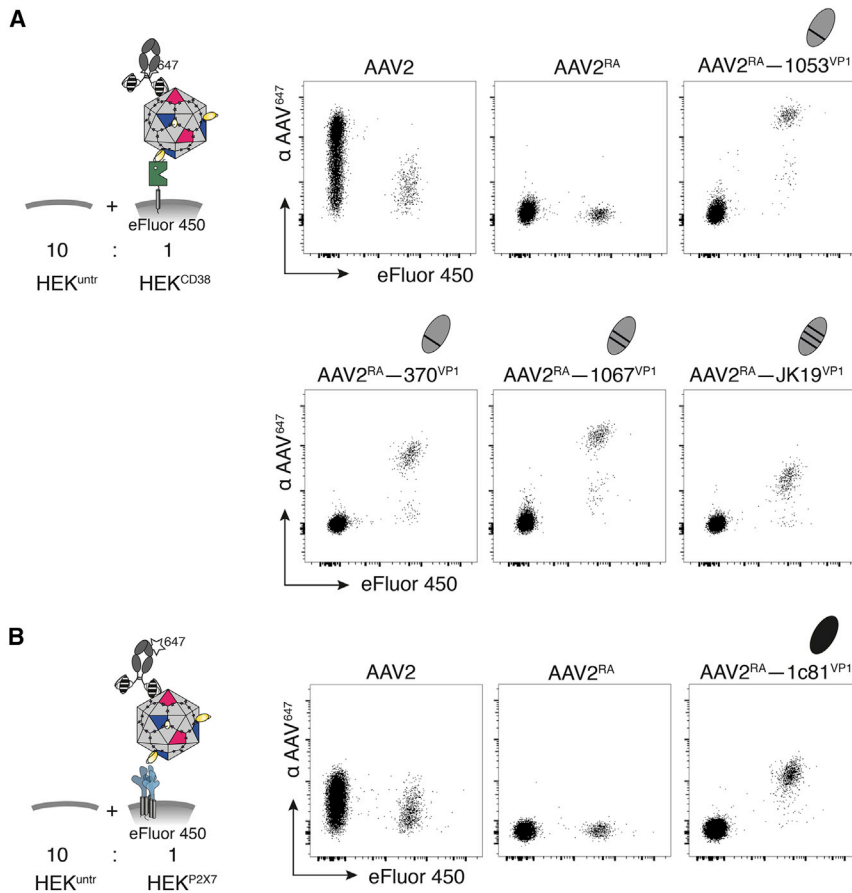


Figure 3. Membrane Protein-Specific Nanobodies Are Readily Incorporated into AAV Capsids and Mediate Specific Binding of Recombinant AAV to Target-Expressing Cells

Untransfected HEK cells were mixed in a ratio of 10:1 with eFluor 450-labeled HEK cells stably transfected with either CD38 (A) or P2X7 (B). Cells were incubated with AAV-containing cell culture supernatants ($\sim 1 \times 10^9$ vector genomes [vg]/100 μ L) for 30 min on ice. Cells were washed to remove unbound AAVs and bound AAVs were detected with Alexa 647-conjugated AAV2-specific scFvA20-rbFc by flow cytometry.

nally with a 25-aa long linker and C-terminally with a 5-aa short linker. During cloning a 7-aa stretch of the VP1 capsid protein (453-GTTTQSR-459) was replaced by a 125- to 145-aa nanobody-targeting domain flanked by linker peptides. Remarkably, the six nanobodies that we inserted at this position were all effectively incorporated into recombinant AAV. Since these nanobodies carry different frameworks and different CDR loops, the GH2/3 loop likely is suited for insertion of a broad range of nanobodies.

GFP and design ankyrin repeat proteins (DAR-Pins) have also been fused successfully to the N terminus of VP2 of AAV2.^{38,39} An Her2-specific DARPin thereby enhanced the transduction of Her2-expressing tumor cells, provided that binding to HSPG was abolished simultaneously by substitution of R585 and R588 with alanine residues.³⁹ Similarly, a CD4-specific DARPin enhanced targeting of human CD4-expressing lymphocytes by AAV2^{RA}.⁴⁰ Fusion to the N terminus of VP2 positions these targeting moieties in a location that is analogous to the PLA2 domain of VP1 (Figure 1C).⁴¹ The PLA2 domain is located on the inner side of the viral capsid facing the viral genome,⁴² and externalization of this domain occurs after endocytosis of the virus into the host cell.^{43,44} Perhaps N-terminal fusion of a DARPin to VP2 forces this part of the protein to externalize during capsid assembly. Consequently, in order to optimize the target cell specificity, Münch et al.⁴⁰ affinity purified DARPin-displaying AAV2 via an N-terminally linked hexahistidine tag. As single immunoglobulin domains of 110- to 130-aa residues, nanobodies are similar in size to both the PLA2 domain of VP1 (137 aa) and to DARPins (14–17 kDa). However, N-terminal fusion of our nanobodies to VP2 did not yield any detectable binding to target-expressing cells (data not shown).

The known AAV serotypes differ substantially in terms of stability, immunogenicity, target specificity, production yield, and transduction efficiency.⁴⁵ Considering that capsid proteins of different AAV serotypes readily assemble into mosaic AAV capsids, we hypothesized that the VP1-nanobody fusion protein strategy could

results show that this strategy can be readily adapted to different AAV serotypes and to structurally different target membrane proteins.

A membrane-specific nanobody has been used previously for retargeting an enveloped lentivirus by stably expressing the nanobody as a transmembrane protein in HEK producer cells.^{33,34} Lentiviruses acquire their envelope from the host cell plasma membrane during budding from the infected cell. For non-enveloped viruses such as AAVs, physical incorporation of a nanobody-targeting moiety into the capsid without compromising virus stability, yield, and infectivity poses a more challenging problem.

Various surface loops of the AAV capsid have been tested for insertion of a peptide-targeting moiety.^{9,35} We introduced the nanobody-targeting moiety into the only site on the surface of AAV2 known to tolerate insertion of a large protein (mCherry, 240 aa, 27 kDa, $\sim 50\%$ larger than nanobodies) without loss of yield or infectivity.³⁰ The N terminus of a nanobody is located close to its antigen-binding paratope on one side of the egg-shaped immunoglobulin domain, while its C terminus is on the opposite side away from its paratope.^{36,37} In order to tether the tail of the nanobody close to the viral capsid while ensuring a flexible, outward-facing orientation of the antigen-binding paratope, we flanked the nanobody N-termi-

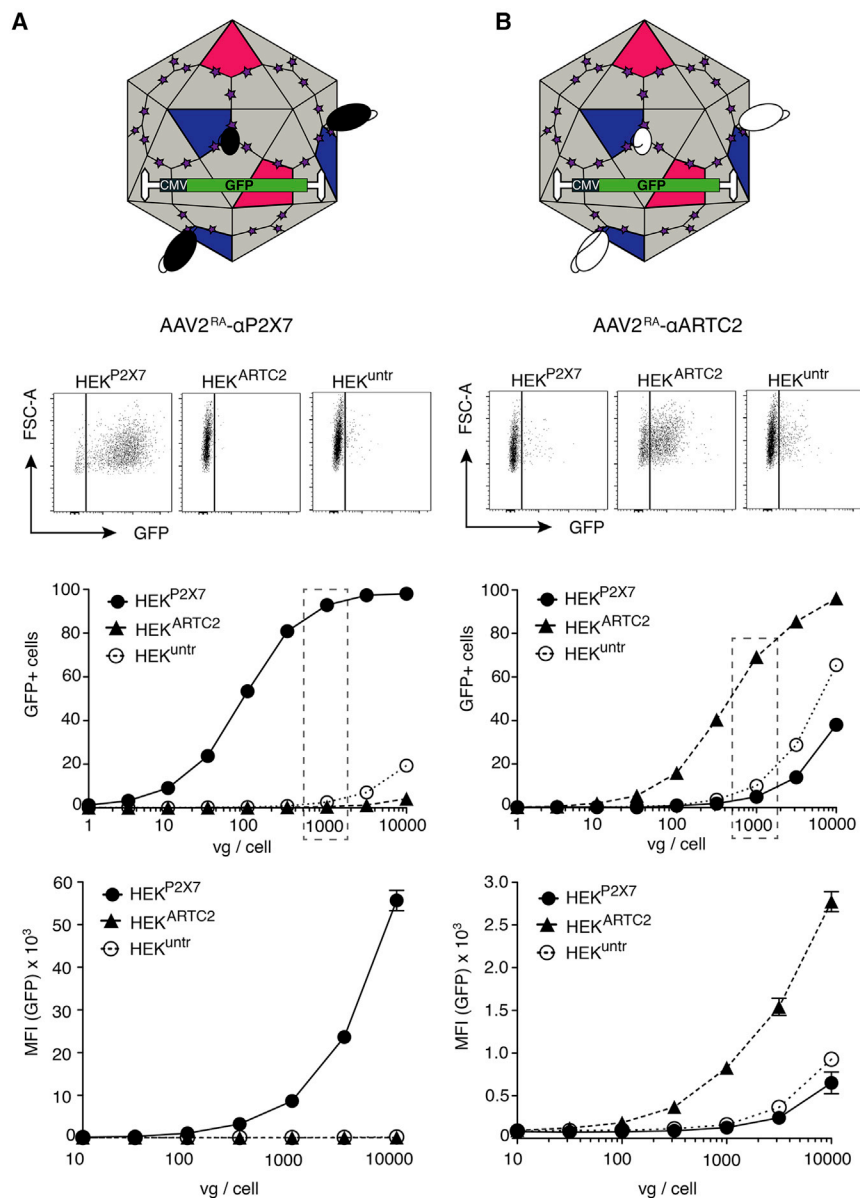


Figure 4. Insertion of a Membrane Protein-Specific Nanobody into VP1 of AAV2^{RA} Enhances the Transduction of Target-Expressing HEK Cells

HEK cells were incubated with titrated amounts of AAV2^{RA} (1–10,000 vg/cell) displaying either the P2X7-specific nanobody 1c81 (A) or the ARTC2-specific nanobody s-14 (B). Expression of GFP was analyzed 48 h after transduction by flow cytometry. Representative FACS dot plots show cells transduced with 1,000 vg per cell (corresponding to the dashed boxes in the diagrams). Data are representative of three independent experiments. Error bars show the SD of three replicates.

Remarkably, our targeting strategy worked for three structurally quite distinct membrane proteins, i.e., a GPI-anchored ectoenzyme, a type II single-span ectoenzyme, and a homotrimeric multispans ion channel. We originally chose these membrane proteins as targets because corresponding nanobodies were available in our laboratory.^{27–29} In each case, we achieved 10- to 500-fold enhanced transduction of target-transfected HEK cells. We achieved similar enhancements also with other target protein-expressing cells, including mouse mammary carcinoma cells, lymphoma cell lines, and primary bone marrow cells endogenously expressing CD38 or P2X7. Neither of these is known to be involved in the endocytic pathway. Considering the current surge of interest in membrane protein-specific nanobodies,^{25,46} it is likely that our targeting strategies can be applied to many different membrane proteins. It is conceivable that some of these will prove even more effective than the examples used herein.

It is difficult to predict whether the efficiency of redirecting tropism of AAV serotypes displaying a membrane protein-specific nanobody in cell culture models will be observed also *in vivo*. Not all AAV vectors can cross physical barriers,

be transferred to other AAV serotypes by forcing the incorporation of one or more VP1-Nb fusion proteins of AAV2^{RA} into the capsid of another serotype. In order to prevent incorporation of unmodified VP1 of the host AAV serotype, we changed the sixth codon of VP1 of the host rep-cap plasmid to a stop codon. Co-transfection with the rep-cap plasmid of AAV2^{RA} VP1-Nb (carrying a mutated splice acceptor signal to prevent incorporation of VP2 or VP3 capsid proteins of AAV2^{RA}) resulted in high yields of mosaic AAV for each of the serotypes tested, confirming that VP1-Nb fusion proteins of AAV2^{RA} can readily be incorporated into different AAV serotypes. All mosaic AAVs markedly enhanced transduction of a broad range of different target-expressing cells, including mouse and human lymphoma cells.

for example the tight vascular endothelium in most tissues after an intravenous administration of AAVs.⁴⁷ The intravenous route might be suited to target intravascular CD38-overexpressing chronic lymphatic leukemia cells,⁴⁸ but less suited to target CD38-overexpressing multiple myeloma cells in bone marrow niches.⁴⁹ The fenestrated endothelium of liver sinusoids is permeable to large protein complexes, and most intravenously injected AAV vectors end up in the liver.^{47,50} Previous studies using DARPIn-displaying AAV2^{RA} *in vivo* demonstrated efficient targeting of both subcutaneous and systemic tumors following a single intravenous administration of recombinant AAV2^{RA} (1.5×10^{10} vector genomes) resulting in 10- to 100-fold more genome copies in tumor tissue than in kidney or liver.^{39,40} Considering the similarity in size of nanobodies and

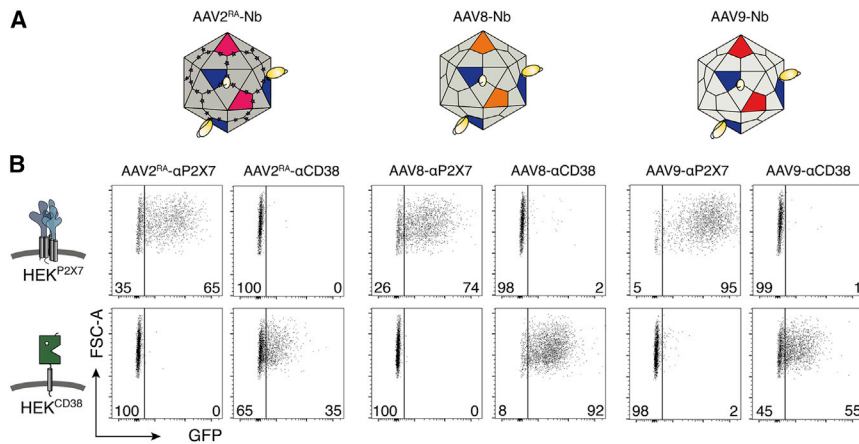


Figure 5. AAV8 and AAV9 Can Be Retargeted by Incorporating a Nanobody-VP1 Fusion Protein of AAV2^{RA}

(A) Schematic diagrams of AAV2^{RA} and mosaic AAV8 or AAV9 carrying a VP1-Nb fusion protein of AAV2^{RA}. (B) P2X7-transfected or CD38-transfected HEK cells were incubated with GFP-encoding AAV2^{RA} or mosaic AAV8 or AAV9 carrying either the P2X7-specific Nb 1c81 or the CD38-specific Nb 1053 (1,000 vector genomes per cell). After 48 h, the cells were analyzed for GFP expression by flow cytometry. Data are representative of three independent experiments.

DARPin, it is not unlikely that these two types of ligand-displaying AAV will show similar *in vivo* pharmacodynamics. Notwithstanding, established strategies to overcome the endothelial barrier by injecting AAV into specific tissues (muscle, peritoneal cavity, retina, cerebrospinal fluid, lung, or tumor mass) may be required to fully harness nanobody-enhanced retargeting of AAV *in vivo*.

Another concern is that the AAV particles may not incorporate the nanobody-VP1 fusion in a uniform manner and that viral particles may be produced that contain only VP2 and VP3. While this is not a major issue in cell culture models, for *in vivo* applications it may be necessary to separate viral particles containing Nb-VP1 fusions from particles composed only of VP2 or VP3. This could be achieved by affinity chromatography on immobilized antigen or protein A (many nanobodies contain a protein A-binding motif).^{37,51} Moreover, the transduction efficiency might be improved further by removal of empty Nb-VP1 capsids from genome-containing capsids, e.g., by anion exchange and/or size exclusion chromatography.^{52,53}

In conclusion, our study provides proof of principle that nanobody technology can be adapted to improve the targeting and transduction efficiencies of AAV vectors.

MATERIALS AND METHODS

Bone Marrow Cells and Cell Lines

Human primary multiple myeloma cells were obtained from bone marrow aspirates after consent was obtained from all patients in accordance with Institutional Review Board approval. Human bone marrow mononuclear cells were prepared by Ficoll-Paque density gradient centrifugation of bone marrow aspirates and subsequent depletion of remaining erythrocytes using red blood cell lysis buffer (NH₄Cl, KHCO₃, EDTA).

HEK293 AAV cells were obtained from Cell Biolabs. The human CA46 lymphoma cell line was obtained from the German Collection of Microorganisms and Cell Culture (DSMZ, Braunschweig, Germany). The murine Yac-1 lymphoma cell line was kindly provided by J. Löhler (Hamburg, Germany). HEK293 cells were kindly pro-

vided by Dr. Carol Stocking (Hamburg, Germany). HEK cells were transfected as indicated with cDNA expression vectors encoding mouse ARTC2.2, mouse P2X7, or human CD38, and stable transfectants were selected by propagation in the presence of a suitable antibiotic and FACS sorting. In cases where two distinct cell populations were mixed for analysis, one of these was labeled with the cell staining dye eFluor 450 (Thermo Fisher Scientific) before mixing. Cells were cultured in DMEM or RPMI 1640 medium (Gibco, Life Technologies, Paisley, UK) supplemented with 2 mM sodium pyruvate (Gibco), 2 mM L-glutamine (Gibco), and 10% (v/v) fetal calf serum (Gibco).

Recombinant Nanobodies and Antibodies

ARTC2.2-specific VHH s-14, CD38-specific VHHs MU1067, MU370, MU1053, and JK19, and P2X7-specific VHH 1c81 were selected from immunized llamas as previously described.^{27–29} The coding sequences of the single-chain variable fragment of mAb A20^{14,31} were generated by gene synthesis (Thermo Fisher Scientific). Nanobody and scFv encoding gene fragments were cloned into the NcoI and NotI sites of the pCSE2.5 vector (kindly provided by Thomas Schirrmann, Braunschweig, Germany) upstream of the coding region for either a chimeric His6x-c-myc peptide tag or the hinge and Fc domains of rabbit IgG1.⁵⁴ Recombinant nanobodies and antibodies were expressed in transiently transfected HEK-6E cells (kindly provided by Ives Durocher, Montreal, QC, Canada) cultivated in serum-free medium. Six days after transfection, supernatants were harvested and cleared by centrifugation.⁵⁵ Nanobodies and antibodies were purified by affinity chromatography using NiNTA agarose or protein A-Sepharose, and purity was assessed by SDS-PAGE and Coomassie brilliant blue staining. Purified nanobodies and antibodies were conjugated to Alexa Fluor 647 or Alexa Fluor 488 via NH₂ esters (Molecular Probes).

Recombinant AAVs

For insertion of a nanobody into the GH2/3 loop of VP1 of AAV2, the VHH-coding region was amplified by PCR using a forward primer encoding an NgoMIV restriction site and a (GGGG)₅ linker and a reverse primer encoding a GGGGA linker and a KsaI restriction site. The PCR fragment was cloned into the NgoMIV and KsaI sites of the rep-cap vector pRC_RR_VP1_r1c3 (kindly provided by Junghee Suh, Rice University, Houston, TX). This vector contains

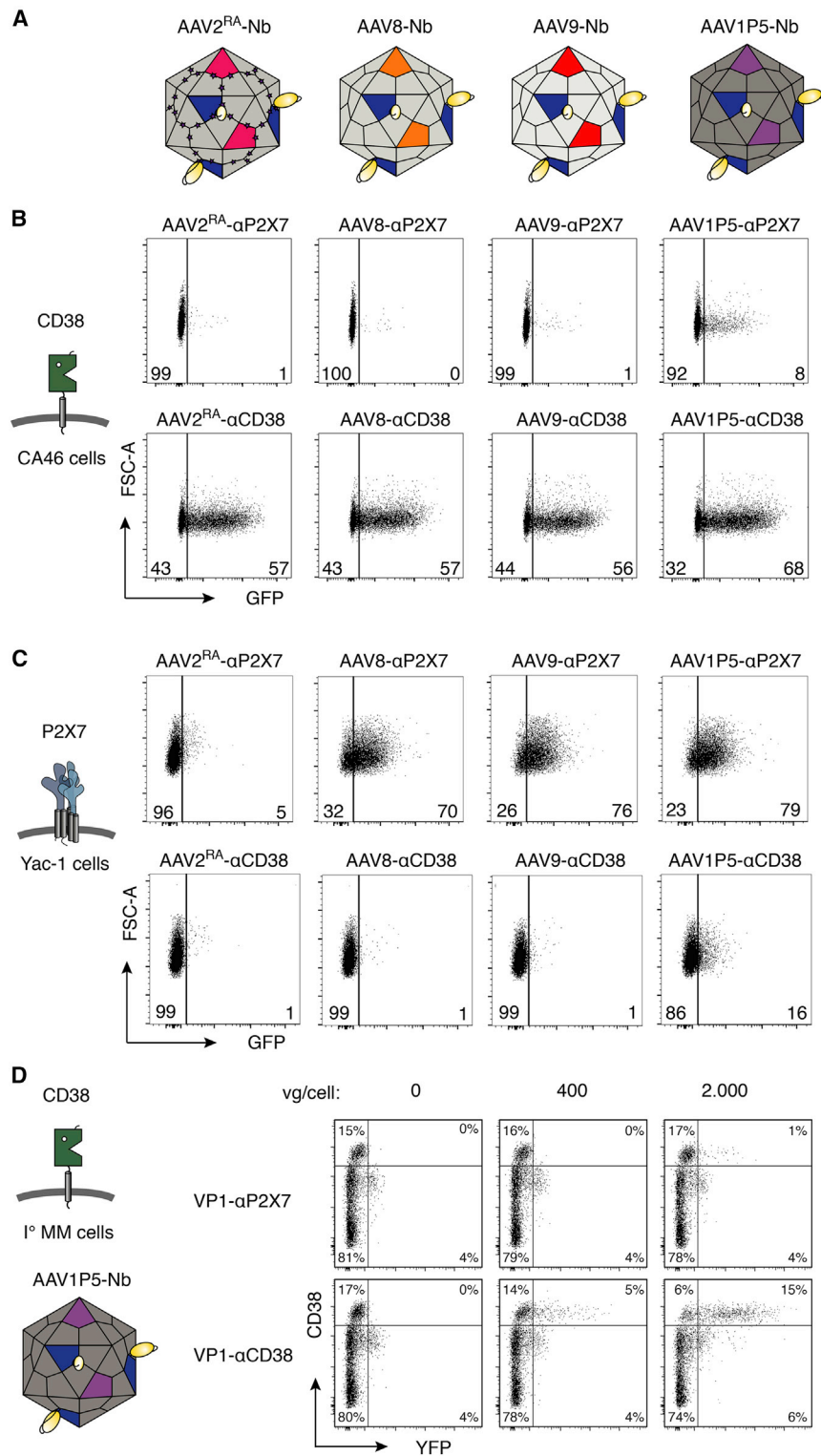


Figure 6. Nanobody-Displaying AAVs Specifically Enhance the Transduction of Target-Expressing Cells

(A) Schematic diagrams of AAV2^{RA} and mosaic AAV8, AAV9, and AAV1P5 carrying a VP1-Nb fusion protein of AAV2^{RA}. Human CA46 Burkitt (B) or mouse Yac-1 (C) lymphoma cells were incubated with the indicated GFP-encoding AAV (1,000 vg/cell). GFP expression was analyzed after 48 h. (D) Primary human bone marrow cells from a multiple myeloma patient were incubated with the indicated GFP-encoding AAV (0–500 vg/cell) and GFP expression was analyzed after 48 h. Data are representative of three (B and C) or two (D) independent experiments.

a mutated splice acceptor signal for the common VP2/VP3 mRNA to prevent production of any VP2-Nb or VP3-Nb fusions.³⁰ The rep-cap vector pRC_RR_VP2-3 containing an inactivated VP1 start codon to allow production of unmodified VP2 and VP3 of AAV2 was also kindly provided by Junghae Suh (Rice University, Houston, TX). Site-directed mutagenesis using the QuikChange II site-directed mutagenesis kit (Agilent Technologies) was used to replace the codons for R585 and R588 of AAV2 with codons for alanine. Similarly, site-directed mutagenesis was used to introduce a stop codon into the sixth codon of VP1 in the rep-cap plasmids encoding AAV1P5, AAV6, AAV8, AAV9, or AAVrh10 (AAV1P5 contains a 9-aa insertion in the GH12/GH13 loop and transduces immune cells more effectively than does parental AAV1 (K. Börner, E. Kienle, L.-Y. Huang, J. Weinmann, A. Sacher, P. Bayer, C. Stüllein, J. Fakhiri, L. Zimmermann, A. Westhaus, J. Beneke, N. Beil, E. Wiedtke, D. Miltnner, A. Rau, T. Erfle, H.-G. Kräusslich, M. Müller, M. Agbandje-McKenna, D. Grimm, unpublished data).

Recombinant AAVs were produced by triple transfection of HEK293 AAV cells (Cell Biolabs), plated at 6×10^6 cells per 15-cm dish in 25 mL of DMEM, 10% fetal calf serum[FCS]) using 20 μ g of helper plasmid pXX6, 4 μ g of reporter-encoding transgene scAAV-CMVeGFP or scAAV-CMVeYFP, and 4.5 μ g of rep-cap plasmid per dish. Recombinant AAV containing VP1-nanobody fusions were produced by quadruple transfection of HEK293 AAV cells using 20 μ g of helper plasmid, 4 μ g of transgene plasmid, and 4.5 μ g of each of rep-cap plasmids encoding either VP1-Nb or VP2/VP3 per dish. The medium was replaced by 17 mL of fresh medium 1 h before transfection. Polyethylenimine (PEI; 25 kDa, Polysciences) was used as transfection reagent at fourfold molar excess to the DNA. After 24 h, the medium was replaced with 25 mL of fresh medium. After 3 days, AAVs were harvested from the cell supernatant and cell lysates.

AAVs were precipitated from the supernatant after overnight incubation with 10% w/v PEG-8000, 1 M NaCl by centrifugation at 4,600 rpm for 30 min. The pellet was resuspended in PBS-MK (1 mM MgCl₂, 2.5 mM KCl₂). Cells were resuspended in PBS-MK and lysed by three cycles of freezing/thawing. DNA in supernatants and lysates was digested with benzonase (Sigma, E1014) for 30 min at 37°C (50 U/mL supernatant or lysate). Remaining insoluble material was eliminated by centrifugation for 15 min at 4,600 rpm. Recombinant AAVs were purified by iodixanol density-gradient ultracentrifugation or via affinity chromatography using AVB Sepharose columns (GE Healthcare) as described previously.²² Viral genome titers were determined by quantitative real-time PCR.

Western Blot Analyses

AAVs were immunoprecipitated using scFvA20-rbFc immobilized on protein G-Sepharose beads. Bound proteins were eluted with SDS-PAGE sample buffer, size fractionated by SDS-PAGE, and transferred to a polyvinylidene fluoride membrane. Capsid proteins were detected with mAb B1³¹ that recognizes a common epitope at the C terminus of all AAV2 capsid proteins.

Flow Cytometry Analyses

Cell surface expression of ARTC2, P2X7, and CD38 was assessed by incubation of cells with c-Myc-tagged nanobodies and Alexa Fluor 647-conjugated mAb 9E10 (anti-c-Myc). AAV bound to HEK cells were detected with Alexa Fluor 647-conjugated scFvA20-rbFc. Samples were washed and analyzed by flow cytometry using a FACSCanto II (BD Biosciences) and FlowJo software (Treestar).

Transduction of Cells with AAV and Assessment of Transduction Efficiency

HEK293 cells, CA46 cells, Yac-1 cells, and bone marrow cells were seeded in 96- or 24-well culture plates (1×10^4 or 1×10^5 cells/well) in culture medium with 10% FCS. After 2 h, chimeric or mosaic AAVs diluted in medium were added to the cells as indicated (always in triplicates). After 48 h, expression of the GFP or yellow fluorescent protein (YFP) was analyzed by flow cytometry using a FACSCanto II or FACSCelesta (BD Biosciences) and FlowJo software (Treestar).

Statistical Analyses

All statistical analyses were performed with the SPSS package and GraphPad Prism 5 software. A p value < 0.05 was considered to be statistically significant. The Student's t test was used for comparison between two groups. In case of three or more groups, one-way ANOVA was used, followed by a *post hoc* analysis with a Bonferroni's test for multiple comparisons.

AUTHOR CONTRIBUTIONS

Conceptualization, A.M.E., M.T., S.A., D.G., and F.K.-N.; Methodology, A.M.E., K.B., and N.B.; Investigation, A.M.E., K.B., B.A., W.S., and N.B.; Writing – Original Draft, A.M.E. and F.K.-N.; Writing – Review and Editing, A.M.E., J.K., M.T., D.G., S.A., and F.K.-N.; Funding Acquisition, A.M.E., K.B., D.G., S.A., and F.K.-N.; Resources, A.M.E., K.B., J.K., and I.B.; Supervision, D.G., S.A., and F.K.-N.

CONFLICTS OF INTEREST

F.H. and F.K.-N. receive a share of antibody sales via MediGate GmbH, a wholly owned subsidiary of the University Medical Center Hamburg-Eppendorf. A.M.E. and F.K.-N. are co-inventors on a patent application on nanobody-based AAV targeting strategies. K.B. and D.G. are co-inventors on a patent application on peptide-modified AAVs. D.G. is a cofounder and shareholder of AaviGen GmbH.

ACKNOWLEDGMENTS

This work was supported by a stipend from the Claussen-Simon-Stiftung to A.M.E., by a grant from the Deutsche Forschungsgemeinschaft to F.K.-N. (310/13-1), by grants from the German Center for Infection Research (DZIF, BMBF) to K.B. and D.G. (TTU-HIV 04.803 and TTU-HIV 04.815), and by a grant from the Agence Nationale de la Recherche to S.A. (ANR-18-CE92-0046). We thank Fabienne Seyfried, Sana Javed (Institute of Immunology, UKE), Björn Rissiek (Department of Neurology, UKE), and Henning Seismann (Department of Oncology, UKE) for excellent technical assistance. We thank Stephan Menzel, Thomas Eden, and Eva Tolosa (Hamburg, Germany) for critical reading of the manuscript. The pCSE2.5

expression plasmid was kindly provided by Thomas Schirrmann (Braunschweig, Germany), HEK-6E cells by Ives Durocher (NRC, Montreal, QC, Canada), and plasmids pRC_RR_VP1-r1c3 and pRC_RR_VP2-3 were provided by Junghae Suh (Rice University, Houston, TX).

REFERENCES

- Mingozzi, F., and High, K.A. (2011). Therapeutic *in vivo* gene transfer for genetic disease using AAV: progress and challenges. *Nat. Rev. Genet.* *12*, 341–355.
- Kotterman, M.A., and Schaffer, D.V. (2014). Engineering adeno-associated viruses for clinical gene therapy. *Nat. Rev. Genet.* *15*, 445–451.
- Colella, P., Ronzitti, G., and Mingozzi, F. (2017). Emerging issues in AAV-mediated *in vivo* gene therapy. *Mol. Ther. Methods Clin. Dev.* *8*, 87–104.
- Balazs, A.B., Ouyang, Y., Hong, C.M., Chen, J., Nguyen, S.M., Rao, D.S., An, D.S., and Baltimore, D. (2014). Vectored immunoprophylaxis protects humanized mice from mucosal HIV transmission. *Nat. Med.* *20*, 296–300.
- Borel, F., Kay, M.A., and Mueller, C. (2014). Recombinant AAV as a platform for translating the therapeutic potential of RNA interference. *Mol. Ther.* *22*, 692–701.
- Yang, Y., Wang, L., Bell, P., McMenamin, D., He, Z., White, J., Yu, H., Xu, C., Morizono, H., Musunuru, K., et al. (2016). A dual AAV system enables the Cas9-mediated correction of a metabolic liver disease in newborn mice. *Nat. Biotechnol.* *34*, 334–338.
- Herrmann, A.K., and Grimm, D. (2018). High-throughput dissection of AAV-host interactions: the fast and the curious. *J. Mol. Biol.* *430*, 2626–2640.
- Foust, K.D., Nurre, E., Montgomery, C.L., Hernandez, A., Chan, C.M., and Kaspar, B.K. (2009). Intravascular AAV9 preferentially targets neonatal neurons and adult astrocytes. *Nat. Biotechnol.* *27*, 59–65.
- Büning, H., Huber, A., Zhang, L., Meumann, N., and Hacker, U. (2015). Engineering the AAV capsid to optimize vector-host-interactions. *Curr. Opin. Pharmacol.* *24*, 94–104.
- Ried, M.U., Girod, A., Leike, K., Büning, H., and Hallek, M. (2002). Adeno-associated virus capsids displaying immunoglobulin-binding domains permit antibody-mediated vector retargeting to specific cell surface receptors. *J. Virol.* *76*, 4559–4566.
- Ponnazhagan, S., Mahendra, G., Kumar, S., Thompson, J.A., and Castillas, M., Jr. (2002). Conjugate-based targeting of recombinant adeno-associated virus type 2 vectors by using avidin-linked ligands. *J. Virol.* *76*, 12900–12907.
- Landegger, L.D., Pan, B., Askew, C., Wassmer, S.J., Gluck, S.D., Galvin, A., Taylor, R., Forge, A., Stankovic, K.M., Holt, J.R., and Vandenberghe, L.H. (2017). A synthetic AAV vector enables safe and efficient gene transfer to the mammalian inner ear. *Nat. Biotechnol.* *35*, 280–284.
- Xie, Q., Bu, W., Bhatia, S., Hare, J., Somasundaram, T., Azzi, A., and Chapman, M.S. (2002). The atomic structure of adeno-associated virus (AAV-2), a vector for human gene therapy. *Proc. Natl. Acad. Sci. USA* *99*, 10405–10410.
- McCraw, D.M., O'Donnell, J.K., Taylor, K.A., Stagg, S.M., and Chapman, M.S. (2012). Structure of adeno-associated virus-2 in complex with neutralizing monoclonal antibody A20. *Virology* *431*, 40–49.
- Xie, Q., Lerch, T.F., Meyer, N.L., and Chapman, M.S. (2011). Structure-function analysis of receptor-binding in adeno-associated virus serotype 6 (AAV-6). *Virology* *420*, 10–19.
- Kern, A., Schmidt, K., Leder, C., Müller, O.J., Wobus, C.E., Bettinger, K., Von der Lieth, C.W., King, J.A., and Kleinschmidt, J.A. (2003). Identification of a heparin-binding motif on adeno-associated virus type 2 capsids. *J. Virol.* *77*, 11072–11081.
- Boucas, J., Lux, K., Huber, A., Schievenbusch, S., von Freyend, M.J., Perabo, L., Quadt-Humme, S., Odenthal, M., Hallek, M., and Büning, H. (2009). Engineering adeno-associated virus serotype 2-based targeting vectors using a new insertion site-position 453-and single point mutations. *J. Gene Med.* *11*, 1103–1113.
- Müller, O.J., Kaul, F., Weitzman, M.D., Pasqualini, R., Arap, W., Kleinschmidt, J.A., and Trepel, M. (2003). Random peptide libraries displayed on adeno-associated virus to select for targeted gene therapy vectors. *Nat. Biotechnol.* *21*, 1040–1046.
- Maheshri, N., Koerber, J.T., Kaspar, B.K., and Schaffer, D.V. (2006). Directed evolution of adeno-associated virus yields enhanced gene delivery vectors. *Nat. Biotechnol.* *24*, 198–204.
- Grimm, D., Lee, J.S., Wang, L., Desai, T., Akache, B., Storm, T.A., and Kay, M.A. (2008). *In vitro* and *in vivo* gene therapy vector evolution via multispecies interbreeding and retargeting of adeno-associated viruses. *J. Virol.* *82*, 5887–5911.
- Deverman, B.E., Pravdo, P.L., Simpson, B.P., Kumar, S.R., Chan, K.Y., Banerjee, A., Wu, W.L., Yang, B., Huber, N., Pasca, S.P., and Gradinaru, V. (2016). Cre-dependent selection yields AAV variants for widespread gene transfer to the adult brain. *Nat. Biotechnol.* *34*, 204–209.
- Körbelin, J., Dogbevia, G., Michelfelder, S., Ridder, D.A., Hunger, A., Wenzel, J., Seismann, H., Lampe, M., Bannach, J., Pasparakis, M., et al. (2016). A brain microvasculature endothelial cell-specific viral vector with the potential to treat neurovascular and neurological diseases. *EMBO Mol. Med.* *8*, 609–625.
- Bartlett, J.S., Kleinschmidt, J., Boucher, R.C., and Samulski, R.J. (1999). Targeted adeno-associated virus vector transduction of nonpermissive cells mediated by a bispecific F(ab')₂ antibody. *Nat. Biotechnol.* *17*, 181–186.
- Hamers-Casterman, C., Atarhouch, T., Muyldermans, S., Robinson, G., Hamers, C., Songa, E.B., Bendahman, N., and Hamers, R. (1993). Naturally occurring antibodies devoid of light chains. *Nature* *363*, 446–448.
- Ingram, J.R., Schmidt, F.I., and Ploegh, H.L. (2018). Exploiting nanobodies' singular traits. *Annu. Rev. Immunol.* *36*, 695–715.
- Wesolowski, J., Alzogaray, V., Reyelt, J., Unger, M., Juarez, K., Urrutia, M., Cauerhff, A., Danquah, W., Rissiek, B., Scheuplein, F., et al. (2009). Single domain antibodies: promising experimental and therapeutic tools in infection and immunity. *Med. Microbiol. Immunol. (Berl.)* *198*, 157–174.
- Danquah, W., Meyer-Schwesinger, C., Rissiek, B., Pinto, C., Serracant-Prat, A., Amadi, M., Iacenda, D., Knop, J.H., Hammel, A., Bergmann, P., et al. (2016). Nanobodies that block gating of the P2X7 ion channel ameliorate inflammation. *Sci. Transl. Med.* *8*, 366ra162.
- Fumey, W., Koenigsdorf, J., Kunick, V., Menzel, S., Schütze, K., Unger, M., Schriewer, L., Haag, F., Adam, G., Oberle, A., et al. (2017). Nanobodies effectively modulate the enzymatic activity of CD38 and allow specific imaging of CD38⁺ tumors in mouse models *in vivo*. *Sci. Rep.* *7*, 14289.
- Koch-Nolte, F., Reyelt, J., Schössow, B., Schwarz, N., Scheuplein, F., Rothenburg, S., Haag, F., Alzogaray, V., Cauerhff, A., and Goldbaum, F.A. (2007). Single domain antibodies from llama effectively and specifically block T cell ecto-ADP-ribosyltransferase ART2.2 *in vivo*. *FASEB J.* *21*, 3490–3498.
- Judd, J., Wei, F., Nguyen, P.Q., Tartaglia, L.J., Agbandje-McKenna, M., Silberg, J.J., and Suh, J. (2012). Random insertion of mCherry into VP3 domain of adeno-associated virus yields fluorescent capsids with no loss of infectivity. *Mol. Ther. Nucleic Acids* *1*, e54.
- Wistuba, A., Weger, S., Kern, A., and Kleinschmidt, J.A. (1995). Intermediates of adeno-associated virus type 2 assembly: identification of soluble complexes containing Rep and Cap proteins. *J. Virol.* *69*, 5311–5319.
- Choi, V.W., McCarty, D.M., and Samulski, R.J. (2005). AAV hybrid serotypes: improved vectors for gene delivery. *Curr. Gene Ther.* *5*, 299–310.
- Goyvaerts, C., De Groeve, K., Dingemans, J., Van Lint, S., Robays, L., Heirman, C., Reiser, J., Zhang, X.Y., Thielemans, K., De Baetselier, P., et al. (2012). Development of the nanobody display technology to target lentiviral vectors to antigen-presenting cells. *Gene Ther.* *19*, 1133–1140.
- Goyvaerts, C., Dingemans, J., De Groeve, K., Heirman, C., Van Gulck, E., Vanham, G., De Baetselier, P., Thielemans, K., Raes, G., and Breckpot, K. (2013). Targeting of human antigen-presenting cell subsets. *J. Virol.* *87*, 11304–11308.
- Büning, H., Ried, M.U., Perabo, L., Gerner, F.M., Huttner, N.A., Ennsle, J., and Hallek, M. (2003). Receptor targeting of adeno-associated virus vectors. *Gene Ther.* *10*, 1142–1151.
- Desmyter, A., Transue, T.R., Ghahroudi, M.A., Thi, M.H., Poortmans, F., Hamers, R., Muyldermans, S., and Wyns, L. (1996). Crystal structure of a camel single-domain VH antibody fragment in complex with lysozyme. *Nat. Struct. Biol.* *3*, 803–811.
- Muyldermans, S. (2013). Nanobodies: natural single-domain antibodies. *Annu. Rev. Biochem.* *82*, 775–797.

38. Warrington, K.H., Jr., Gorbatyuk, O.S., Harrison, J.K., Opie, S.R., Zolotukhin, S., and Muzyczka, N. (2004). Adeno-associated virus type 2 VP2 capsid protein is nonessential and can tolerate large peptide insertions at its N terminus. *J. Virol.* **78**, 6595–6609.
39. Münch, R.C., Janicki, H., Völker, I., Rasbach, A., Hallek, M., Büning, H., and Buchholz, C.J. (2013). Displaying high-affinity ligands on adeno-associated viral vectors enables tumor cell-specific and safe gene transfer. *Mol. Ther.* **21**, 109–118.
40. Münch, R.C., Muth, A., Muik, A., Friedel, T., Schmatz, J., Dreier, B., Trkola, A., Plückthun, A., Büning, H., and Buchholz, C.J. (2015). Off-target-free gene delivery by affinity-purified receptor-targeted viral vectors. *Nat. Commun.* **6**, 6246.
41. Girod, A., Wobus, C.E., Zádori, Z., Ried, M., Leike, K., Tijssen, P., Kleinschmidt, J.A., and Hallek, M. (2002). The VP1 capsid protein of adeno-associated virus type 2 is carrying a phospholipase A2 domain required for virus infectivity. *J. Gen. Virol.* **83**, 973–978.
42. Kronenberg, S., Böttcher, B., von der Lieth, C.W., Bleker, S., and Kleinschmidt, J.A. (2005). A conformational change in the adeno-associated virus type 2 capsid leads to the exposure of hidden VP1 N termini. *J. Virol.* **79**, 5296–5303.
43. Sonntag, F., Bleker, S., Leuchs, B., Fischer, R., and Kleinschmidt, J.A. (2006). Adeno-associated virus type 2 capsids with externalized VP1/VP2 trafficking domains are generated prior to passage through the cytoplasm and are maintained until uncoating occurs in the nucleus. *J. Virol.* **80**, 11040–11054.
44. Stahnke, S., Lux, K., Uhrig, S., Kreppel, F., Hösel, M., Coutelle, O., Ogris, M., Hallek, M., and Büning, H. (2011). Intrinsic phospholipase A2 activity of adeno-associated virus is involved in endosomal escape of incoming particles. *Virology* **409**, 77–83.
45. Bennett, A., Patel, S., Mietzsch, M., Jose, A., Lins-Austin, B., Yu, J.C., Bothner, B., McKenna, R., and Agbandje-McKenna, M. (2017). Thermal stability as a determinant of AAV serotype identity. *Mol. Ther. Methods Clin. Dev.* **6**, 171–182.
46. Eden, T., Menzel, S., Wesolowski, J., Bergmann, P., Nissen, M., Dubberke, G., Seyfried, F., Albrecht, B., Haag, F., and Koch-Nolte, F. (2018). A cDNA immunization strategy to generate nanobodies against membrane proteins in native conformation. *Front. Immunol.* **8**, 1989.
47. Zincarelli, C., Soltys, S., Rengo, G., and Rabinowitz, J.E. (2008). Analysis of AAV serotypes 1–9 mediated gene expression and tropism in mice after systemic injection. *Mol. Ther.* **16**, 1073–1080.
48. Burgler, S. (2015). Role of CD38 expression in diagnosis and pathogenesis of chronic lymphocytic leukemia and its potential as therapeutic target. *Crit. Rev. Immunol.* **35**, 417–432.
49. Morandi, F., Horenstein, A.L., Costa, F., Giuliani, N., Pistoia, V., and Malavasi, F. (2018). CD38: a target for immunotherapeutic approaches in multiple myeloma. *Front. Immunol.* **9**, 2722.
50. Kattenhorn, L.M., Tipper, C.H., Stoica, L., Geraghty, D.S., Wright, T.L., Clark, K.R., and Wadsworth, S.C. (2016). Adeno-associated virus gene therapy for liver disease. *Hum. Gene Ther.* **27**, 947–961.
51. Graille, M., Stura, E.A., Corper, A.L., Sutton, B.J., Taussig, M.J., Charbonnier, J.B., and Silverman, G.J. (2000). Crystal structure of a *Staphylococcus aureus* protein A domain complexed with the Fab fragment of a human IgM antibody: structural basis for recognition of B-cell receptors and superantigen activity. *Proc. Natl. Acad. Sci. USA* **97**, 5399–5404.
52. Urabe, M., Xin, K.Q., Obara, Y., Nakakura, T., Mizukami, H., Kume, A., Okuda, K., and Ozawa, K. (2006). Removal of empty capsids from type 1 adeno-associated virus vector stocks by anion-exchange chromatography potentiates transgene expression. *Mol. Ther.* **13**, 823–828.
53. Tomono, T., Hirai, Y., Okada, H., Miyagawa, Y., Adachi, K., Sakamoto, S., Kawano, Y., Chono, H., Mineno, J., Ishii, A., et al. (2018). Highly efficient ultracentrifugation-free chromatographic purification of recombinant AAV serotype 9. *Mol. Ther. Methods Clin. Dev.* **11**, 180–190.
54. Schirrmann, T., and Büsow, K. (2010). Transient production of scFv-Fc fusion proteins in mammalian cells. In *Antibody Engineering, Volume 2*, R. Kontermann and S. Dübel, eds. Antibody Engineering (Springer-Verlag), pp. 387–398.
55. Zhang, J., Liu, X., Bell, A., To, R., Baral, T.N., Azizi, A., Li, J., Cass, B., and Durocher, Y. (2009). Transient expression and purification of chimeric heavy chain antibodies. *Protein Expr. Purif.* **65**, 77–82.